Plasmonic mode analysis on an embedding periodic solid/outline bowtie nanoantenna array in a substrate

Yuan-Fong Chau [1+]

[1] Department of Electronic Engineering, Chien Hsin University of Science and Technology, No.229, Jianxing Rd., Zhongli City, Taoyuan County 32097, Taiwan (R.O.C.)

Abstract. Plasmonic effects of a periodic outline bowtie nanoantenna array (POBNA) which is embedded in a substrate with different depths is numerically investigated by using the finite element method. The electromagnetic modes obtained from the embedding cases are quite different from that of the free standing cases of their counterparts, resulting in an intensity enhancement and a redshift phenomenon. Simulation results show that the embedded depth of the POBNA in a silica substrate is a key role on the field enhancement and the position of peak resonant wavelengths.

Keywords: Plasmonic Effects, Bowtie Nanoantenna Array, Finite Element Method

1. Introduction

Rescently, plasmonic nanoantennas (PNAs) [1-3] have attracted of great interest by researchers owing to their potential to support the localized surface plasmon resonance (SPR) and provide the confined and enhanced electromagnetic fields. PNA consists of two strongly coupled metal nanoparticles (MNPs) which can serve as a model system to study the impact of mode selectivity. Various applications of PNAs have been proposed and demonstrated [3-4]. Besides, their applications can be used in imaging and biological sensing. These PNAs can be used to manipulate MNPs that are attracted by the high intense fields generated in the gap between the MNP regions. The optical properties of different types of PNAs have been discussed over the last few years (see, for example [1, 3, 5-6]). In our previous paper, we first proposed a bowtie PNA with a dielectric core enclosed by a silver film to tune the peak resonant wavelength (λres) of the PNA [3]. The drawback of our proposed design in [3] is that it would require the complex procedures to fabricate them [1]. Thus, in the view point of fabrication and cost, the solid bowtie PNA [2] and outline bowtie PNA [1] are the best choice in this issue.

When a solid/outline bowtie PNA is embedded in an air background and is illuminated with the incident wave of preferential wavelengths, the PNA will be strongly polarized and the incident fields can be enhanced by several orders of magnitude in the PNA gap [7,8]. Usually, the MNPs are put on or embedded in the dielectric substrate. The plasmonic effects of a periodic solid/outline bowtie PNA array embedded in a dielectric substrate have never been widely investigated. In this paper, we numerically investigate a periodic array of solid/outline bowtie PNA which is composed of a pair of identical triangular gold. We will examine the influence of its embedded depths in a silica substrate on the PNA resonance conditions compared to the air background case of its counterpart. Numerical simulations are performed by using three-dimensional (3-D) finite element method (FEM). We examine the near field properties on the PNA resonance conditions at peak wavelengths of interest. In addition, the characteristics of transmittance spectral of the proposed periodic PNA array corresponding to their bonding mode and anti-bonding mode are investigated as well.

[+] Corresponding author. Tel.: + 886-3-4581196 ext 5105; fax: +886-3-4588924.
E-mail address: yfc01@uch.edu.tw.

2. Method, Model, Results and Discussion

The structure of a unit cell of the periodic solid bowtie nanoantenna array (PSBNA) investigated here can be characterized by seven parameters (a, b, c, e, g, X, Y) as shown in Fig. 1(a): the gap width, g; the antenna length along x-axis, a; the antenna width along y-axis, b; the antenna thickness, c and the period along x and y axis, X and Y, respectively. The area of gap region g×e=30 nm × 30 nm is chosen for this study. In addition, the period along x and y axis and gold film thickness are kept constant of X=Y=775 nm and c = 35 nm, respectively. In this paper, we also consider the periodic outline bowtie nanoantenna array (POBNA) which unit cell consisting of a pair of metallic triangular outlines by night parameters (a, b, c, e, g, X, Y, t, d), as shown in Fig. 1(b), with additional structure parameters: the outline thickness, t, and the distance away from vertical edge, d. The dielectric constants of gold were obtained from literature [9]. An antenna flare angle of 90 ° is used, such that a=b. In each simulation, a unit cell of PSBNA/POBNA is embedded in the air background or embedded with a depth of v nm in a fused silica (ns=1.5) substrate (see Fig. 1(c)), where the interface between air and silica substrate is set to be zero (i.e., the origin of the coordinate system is placed at the center of gold/silica interface), while positive v and minus v denote the distance between the top surface of antenna and the interface (top surface of silica). The amplitude of the incident light is set to be 1 V/m throughout this paper. We define a term "gap enhancement" which means the near-field intensity measured at the gap region. In our simulations, we use 3-D FEM, with free tetrahedral high-order edge elements. On the surface of outer simulation region, the case of a unit cell of the PSBNA/POBNA is enclosed by the anisotropic perfectly matched layers (PML) in order to avoid the reflective fields from the boundary of the computational domain. For simulating the PSBNA/POBNA, we set periodic boundary condition (PBC) along the side walls and PML condition on the top and bottom surfaces in order to save the computer resource and simulation time.

First, we investigate the difference of the gap enhancement vs. wavelengths obtained from an air background case of PSBNA and several embedding cases of POBNA with varying the embedded depths in a silica substrate ranging in -10 nm<v<35 nm as shown in Figs. 2 (a) and 2(b), respectively. In our calculations, an x-polarized electromagnetic incident wave launches from the bottom face of the substrate and propagates along the positive z direction (k-direction), which is used to excite the local field surrounding the surface of POBNA (see the inset of Fig. 1). The geometry parameters are used as follows: d=e=30 nm, a=b=500 nm, c=35 nm and t=20 nm, respectively. The SPRs significantly increase the field enhancement within the PNA gap and PNA surface. As shown in Fig. 2(a) that at least two distinct resonance peaks corresponding to the SPR mode can be found. Figure 2(b) also shows the enlarged diagram of Fig. 2(a) which wavelengths are in the range of 0.3-1.5 μm. It is evident in Fig. 2 that the peak resonance wavelength (λres) of the POBNA is always at a longer wavelength when the embedded depth v is increased and λres redshifts to longer wavelengths and the gap enhancement is decreased owing to absorption effects of the dielectric substrate (silica). The second λres shifts from 1.14 μm (for air background case) to 1.68 μm (for case v=-10 nm) and a distinct redshift of 440 nm is obtained. This phenomenon can be explained by the polarization effects of the silica substrate and by the plasmonic effects arising from the interaction between the PNA and the applied incident field, which will be discussed in Fig. 5. Note that the gap enhancements of the embedding cases of POBNA revealed in Fig. 2(b) are achieved a value above 2×10^8 as the incident wavelengths larger than 0.775 μm.

Figure 2(c) shows the difference of the transmittance vs. incident wavelengths obtained from an air background case of PSBNA and several embedding cases of POBNA with varying the embedded depths of PNA in a silica substrate ranging in -10 nm<v<35 nm, whereas the enlarged diagram of Fig. 2(c) which incident wavelengths ranging in 0.3-2.0 μm is displayed in Fig. 2(d). It can be seen from Figs. 2(c) and 2(d) that three different transmittance modes can be found, i.e., mode 1, 2, 3 (term them as mode 1, 2 and 3 hereafter), as indicated in the enclosed dashed-lines of Fig. 2(c) and 2(d). The corresponding transmittance modes and their charge distributions are also displayed in Figs. 3 (a)-(c), respectively. A quite different field patterns and charge distributions can be found, showing bonding [see mode 1, Fig. 3(c)] and anti-bonding [see mode 2 and 3, Fig. 3(a) and 3(b)] mode patterns. Comparison of the results obtained from Figs. 2(c) with 2(d), the transmittance dips in mode 1 are much deeper than those of mode 2 and 3, and redshifts towards longer wavelengths as the decreasing value of v. These results in the splitting of the plasmon mode

into two resonance modes, which are the low energy "bonding" mode (mode 1) and the high energy "anti-bonding" mode (mode 2 and 3). Because of coupling effects between two gold MNPs of the bowtie PNA, we find that the electric field is enhanced and forms a hot spot in the gap for modes 1-3 (see the bottom part of Figs. 3(a)-(c)).

Regarding the direction of electric field propagation (cyan arrows in the bottom part of Figs. 3(a)-3(c)), the schematic charge density of the mode 1-3 are also depicted in the upper part of Figs. 3(a)-3(c), respectively. In mode 1 case, the charge density (see Fig. 3(c)) on the surfaces of the PNA are divided into two parts in the form of dipole arrangement and the charge intensity are stronger than that of mode 2 and 3 cases, showing strong dipole-like charge distributions and resulting in bonding mode resonance. Turning to the mode 2 and 3 cases (see Fig. 3(a) and 3(b)), the charge densities distribute more than two areas and exhibit weaker dipole-like than that of mode 1, leading to an anti-bonding mode resonance. The mechanism on above-mentioned phenomena can be attributed to the symmetries of the positive-negative charge distributions and their distribution profile for gold bowtie PNA arrays. The dipole moments on the PNA surfaces of outline are arranged. A stronger coupling will lead to a new scheme of polarization and result in a thin metallic layer, which could be described as symmetric and asymmetric modes.

When the POBNA/PSBNA is aligned along a particular direction, the symmetry of the system is broken, and proper modes can be found for light polarized parallel to the chain axis of the POBNA/PSBNA. Independently of the direction of the applied field, the spectrum is always red-shifted as the PNAs approaching and embedding the substrate [10]. This can be explained using the real and image charge model as depicted in Figs. 4 (models of the induced local field for an applied field parallel to the POBNA/PSBNA). Figs. 4(a)–4(f) represent the case of v=-10 nm (i.e., the distance between top surface of POBNA/PSBNA and the interface) corresponding to mode 1, 2 and 3, respectively. It can be clearly seen in Figs. 4(a)–4(f) that the induced local electric field Eind is opposite to the external field Eext. When the external field is applied parallel to the interface, it polarizes the particle in the opposite direction to the substrate polarization, thus the induced local field acting on the particle is also along the applied field, such that, the induced local field Eind is in the opposite direction as the applied field, see Fig. 4(a)–4(f), and against the restoring forces, thus resulting the phenomenon of redshift (i.e., increasing the wavelength of the SPRs).
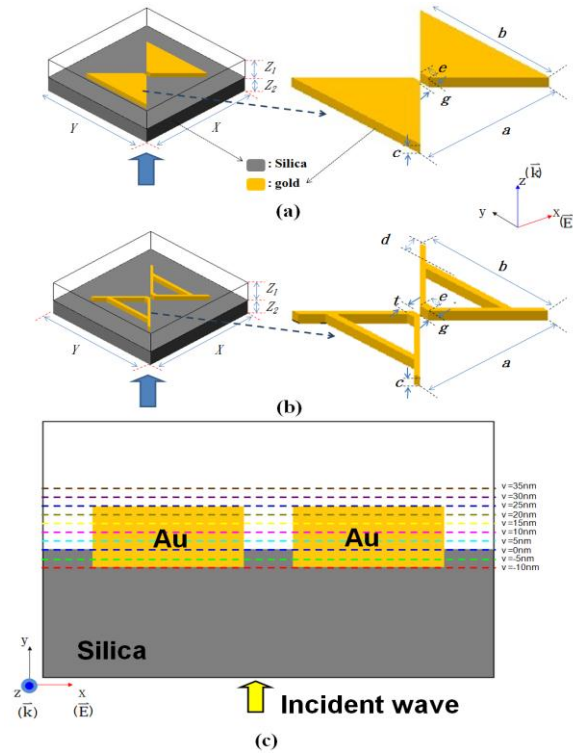

Fig. 1. Schematic of the simulation model. (a) a unit cell of PSBNA with period X=Y on a silica substrate. (a) a unit cell of a POBNA. (c) Side view of an antenna embedded in a silica substrate. The positive v denotes the distance between the antenna and silica, while minus v denoting the embedded depth of the antenna. The dashed lines exactly
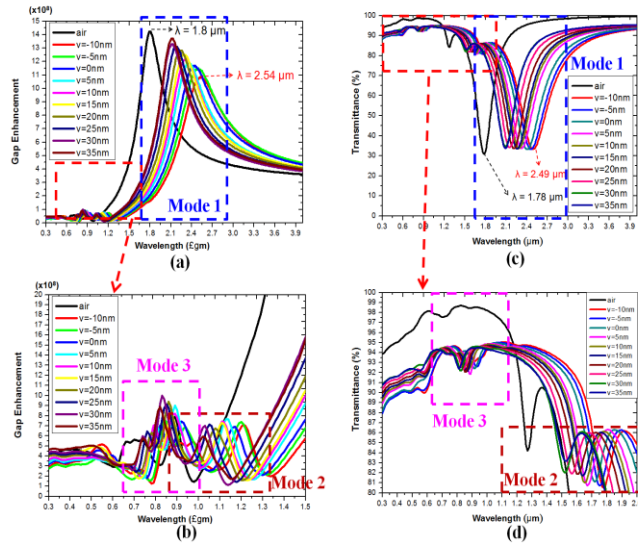
touch the top surface of the antenna.

Fig. 2. (a) Difference of the gap enhancement vs. wavelengths obtained from a PSBNA case (black line) in air background and POBNA cases with varying the embedded depths in a silica substrate ranging in -10<v<35 nm. (b) The enlarged diagram of Fig. 2(a) which incident wavelengths ranging in 0.3-1.5μm. (c) Difference of the transmittance vs. wavelengths obtained from a PSBNA case (black line) in air background and embedding POBNA cases with varying the embedded depths in a silica substrate ranging in -10 nm<v<35 nm. (d) The enlarged diagram of Fig. 2(c) which incident wavelengths ranging in 0.3μm -2.0μm
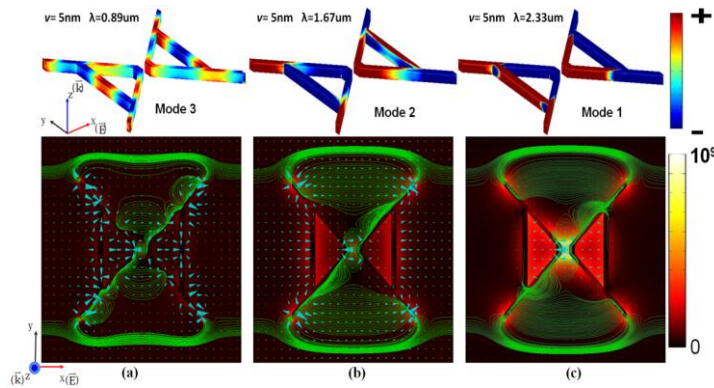

Fig. 3. Corresponding charge distributions and their transmittance modes of mode 1-3. (a) Mode 3, (b) Mode 2, (c) Mode 1, respectively. Where the green lines denote the stream lines (electric force lines).
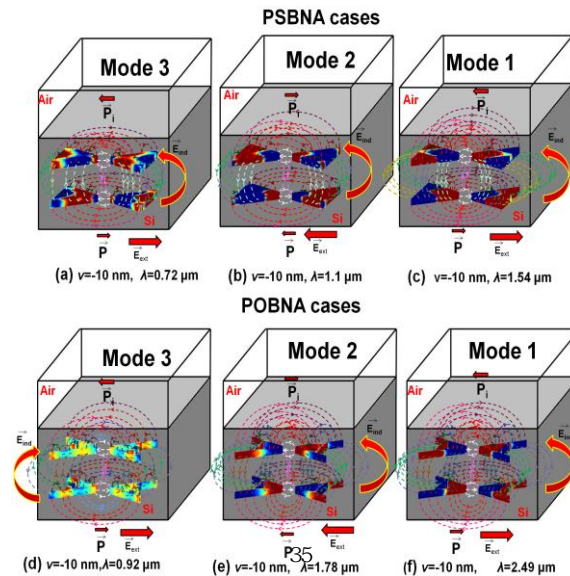

P35

Fig. 4. Models of the induced local field for an applied field parallel to the PSBNA/PSBNA for a selected case of v=-10 nm. (a)-(c) represent the POBNA with embedded depth of v=-10 nm corresponding to mode 1, 2 and 3, respectively. (a)mode 3, λ_{res}=0.72 µm, (b) mode 2, λ_{res}=1.1 µm, (c) mode 1, λ_{res}=1.54 µm. (d)-(f) represent the PSBNA with embedded depth of v=-10 nm corresponding to mode 1, 2 and 3, respectively. (d) mode 1, λ_{res}=0.67 µm, (e) mode 1, λ_{res}=0.95 µm, (f) mode 1, λ_{res}=1.33 µm.

3. Conclusion

In summary, we have numerically investigated the near field properties and plasmonic effects of a periodic solid/outline bowtie PNA array embedded in a substrate with different depths by using FEM with 3-D calculations. The gap enhancement, transmittance, charge distribution and the real and image charge model have been investigated and discussed in our 3-D calculations. Results show that the investigated PNA embedding with different depths in a silica substrate, offering more compact dimensions and a broader spectral while maintaining a constant PNA size.

4. References

[1] Sederberg S, Elezzabi AY, "Nanoscale plasmonic outline bowtie antenna operating in the mid-infrared," Opt. Express, Vol. 19, pp. 15532-15537, 2011.

[2] Jer-Shing Huang, Johannes Kern, Peter Geisler, Pia Weinmann, Martin Kamp, Alfred Forchel, Paolo Biagioni, and Bert Hecht, " Mode Imaging and Selection in Strongly Coupled Nanoantennas," Nano Lett., Vol. 10, pp. 2105–2110, 2010.

[3] Chau YF, Yeh HH, Tsai DP, "A new type of optical antenna: plasmonics nanoshell bowtie antenna with dielectric hole," J. Electromagn. Waves Appl., Vol. 24, pp. 1621–1632, 2010.

[4] Chau YF, Yeh HH, "A comparative study of solid-silver and silver-shell nanodimers on surface Plasmon resonances," J. Nanopart. Res. 13, 637–644, 2011.

[5] Leveque, G. and O. J. F. Martin, "Tunable composite nanoparticle for plasmonics," Opt. Lett., Vol. 31, pp.2750-2752, 2006.

[6] Alu, A. and N. Engheta,"Tuning the scattering response of optical nanoantennas with nanocircuit loads," Nature Photonics, Vol. 2, pp.307-309, 2008.

[7] Neubrech F, Pucci A, Cornelius TW, Karim S, Garcia-Etxarri A, Aizpurua J, "Resonant Plasmonic and Vibrational Coupling in Tailored Antenna for Infrared Detection," Phys. Rev. Lett., Vol. 101, pp. 157403, 2008.

[8] Chau YF, Yeh HH, Liao CC, Ho H F, Liu CY, Tsai DP (2010) Controlling surface plasmon of several pair arrays of silver-shell nanocylinders. Appl. Opt. 49, 1163-1169.

[9] Johnson PB, Christy RW (1972) Optical constants of the noble metals. Phys Rev B 6:4370–4379.

[10] Noguez C, "Surface Plasmons on Metal Nanoparticles: The Influence of Shape and Physical Environment," J Phys Chem C 111, pp. 3806–3819, 2007.